

## Five models for myosin V

Andrej Vilfan<sup>1</sup>

<sup>1</sup>*J. Stefan Institute, Jamova 39, 1000 Ljubljana, Slovenia*

### TABLE OF CONTENTS

1. Abstract	
2. Introduction	
3. Main findings	
3.1. Stepping	
3.2. Step size	
3.3. Force-velocity relation	
3.4. Processivity	
3.5. Kinetics	
3.5.1. Single-headed	
3.5.2. Double-headed	
4. Open questions	
4.1. Head-head coordination	
4.2. Lead head state	
4.3. Sub-steps	
4.4. How tight is the coupling between the hydrolysis cycle and the stepping?	
4.5. Source of elasticity	
5. Theoretical models	
5.1. Overview	
5.2. Discrete stochastic models	
5.2.1. Kolomeisky and Fisher	
5.2.2. Skau, Hoyle and Turner	
5.2.3. Wu, Gao and Karplus	
5.3. Mechano-chemical models	
5.3.1. Lan and Sun	
5.3.2. Elastic lever arm model	
6. Conclusions	
7. Acknowledgements	
8. References	

## 1. ABSTRACT

Myosin V was the first discovered processive motor from the myosin family. It has therefore been subject of a number of mechanical, kinetic, optical and structural studies and now belongs to the best characterised motor proteins. This effort has been accompanied by a number of different theoretical models. In this article we give an overview of them and discuss what they have in common and where the open questions are. The latter include the existence of sub-steps, the process that limits the run length, the nature of backward steps, the flexibility of the lever arm and the state of the lead head.

## 2. INTRODUCTION

Myosin V is a two-headed processive motor protein from the myosin superfamily (1), involved in different forms of intracellular transport (2,3). In 1999 it was shown to be the first processive motor from the myosin superfamily (4). Processivity means that a single molecule can move over a long distance (typically a micron) along an actin filament without dissociating. This discovery came as a surprise, because processivity was only known for microtubule-based motors (kinesin, ncd and cytoplasmic dynein) before. The second feature that makes myosin V unconventional is its long step size around 35 nm (4). After

## Five models for myosin V

myosin V, other processive myosins have been discovered (VI (5), VIIa (6), XI (7), X (8) and according to some evidence IXb (9)), but the amount of knowledge gained on myosin V has made it one of the best, if not the best understood motor protein.

The experiments have characterised it mechanically (usually using optical tweezers) (4,10-16), biochemically (17-20), optically (21-23) and structurally (24-27). These studies have shown that myosin V walks along actin filaments in a hand-over-hand fashion (23,28) with an average step size of about 35 nm, roughly corresponding to the periodicity of actin filaments (4,11,12,21,24), a stall force of around 2.5 pN (11) and a run length of a few microns (11,29,30). Under physiological conditions, ADP release has been identified as the time limiting step in the duty cycle (11,17), which means that the motor spends most of its time waiting for ADP release from the trail head.

Myosin V contains a head domain, which has a high degree of similarity with other myosins like myosin II (muscle myosin). However, there are important differences in the kinetics of the ATP hydrolysis cycle – notably the slow release of ADP, which is necessary for maintaining processivity. The head is connected with a lever arm (also called neck), consisting of an alpha helix, surrounded by six light chains. This is followed by the tail domain, which is responsible for the dimerisation of the molecule and for cargo binding.

Meanwhile the literature on myosin V counts about a dozen of reviews, concentrating on different aspects of myosin V, such as its cellular function and phylogeny (1-3,31-35), regulation (34,36), structure (37) and stepping mechanism (35,38-43). It is not the purpose of this article to review all important findings on myosin V in general, but rather to concentrate on theoretical models and those experimental results they aim at explaining. More specifically, we will critically review 5 existing theoretical models (44-48) and discuss which of them is in agreement with which of the experimental results and where the discrepancies are.

The structure of this paper is as follows. In Section 3 we summarise those experimental results that are most relevant for theoretical models. Section 4 describes some of the most important open questions in the field – particularly those that need cooperation between theory and experiment to be resolved. Section 5 then reviews five theoretical models for the stepping kinetics and mechanics of myosin V. Finally, we give a brief summary and try to project how the different approaches might converge in near future.

## 3. MAIN FINDINGS

The main findings gained with optical tweezers, fluorescent microscopy and chemical kinetics can be summarised as follows:

### 3.1. Stepping

Myosin V walks in a *hand-over-hand fashion* along actin filaments (23,28), as shown in Figure 1A. The lead head performs free Brownian motion around the

common hinge while searching for the new binding site (49,50).

### 3.2. Step size

The *step size* roughly corresponds to the actin periodicity of 35nm (51). The most precise way to determine the *average* step size is by measuring the pitch of the slightly helical motion of the stepping myosin V molecule around the actin filament (21). The *distribution* of step sizes can be determined from EM images (24). The study shows the highest probability for 13 subunit steps (36nm), followed by 15 subunit and 11 subunit steps (Figure 1B).

### 3.3. Force-velocity relation

The *force velocity relation*, shown in Figure 2, reveals the following phases:

Under saturating ATP concentrations (in the millimolar range), the velocity is about 400nm/s and is nearly constant up to loads of about 1pN (16,51). For higher loads, the velocity drops rather sharply and flattens near stall (16,51).

Above the stall force, when the motor is pulled backwards by the load, its velocity increases roughly linearly with the applied load; it reaches around -150nm/s (15) to -250nm/s (14) under 5pN load and around -700nm/s under 10pN (15).

Forward loads only lead to a slight increase in velocity (14,15).

Under low ATP concentrations, the velocity becomes proportional to the ATP concentration and is independent of load between -10pN and 2pN (15,16,51). For super-stall loads, the velocity becomes independent of the ATP concentration.

The stall force of myosin V has been reported as 3pN (4), 2.5-3pN (16), up to 2.5pN (52), but also lower values around 1.7pN (14). Because of short run lengths, some care has to be taken when determining the force-velocity relation close to stall force, as pointed out by Kolomeisky *et al.* for kinesin (53).

Added ADP has a similar effect on the force-velocity curve as a reduced ATP concentration (11,16,30). Added inorganic phosphate in high concentrations (40mM) causes a less significant, but detectable velocity decrease (30,49).

### 3.4. Processivity

The second important source of data is the degree of processivity, usually measured with the average *run length*, i.e., the average distance a single myosin V motor moves along an actin filament before dissociating from it. There is still some discrepancy with regard to the run length of unloaded motors. The first measurement was carried out by Mehta *et al.* (4), who estimated it as 2µm. Veigel *et al.* (12) obtained 2.4 µm, Ali *et al.* (21) 2.1 µm,

## Five models for myosin V

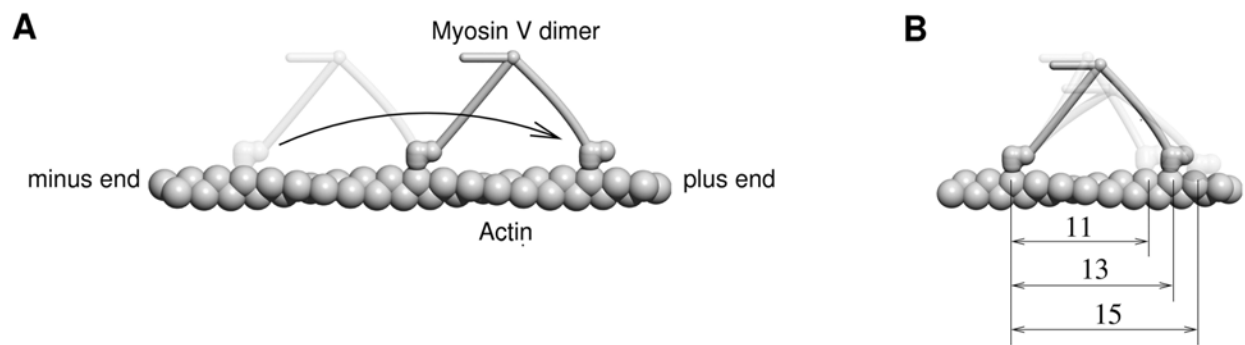


**Figure 1.** (A) Myosin V steps in a hand-over-hand fashion along actin filaments. (B) The most frequent step size is 13 actin subunits, but it can also be 11 and 15 subunits occur.

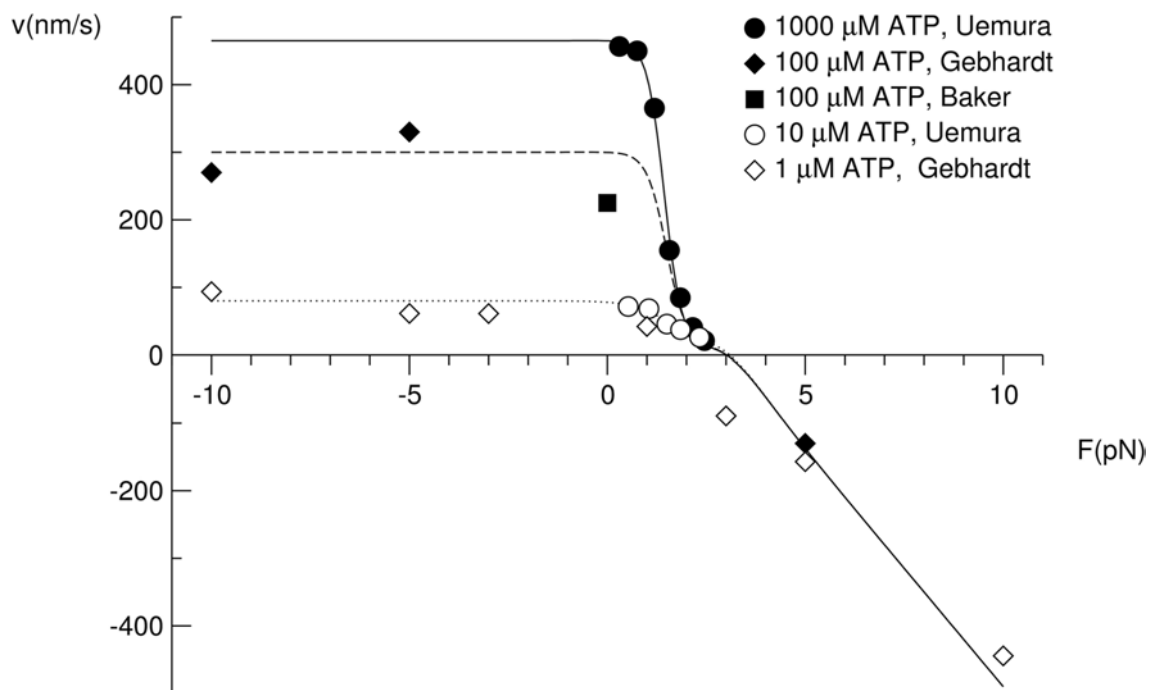


**Figure 2.** Force-velocity relation of myosin V for different ATP concentrations. Data points are taken from Refs. (15), (16), (30). The lines are guide to the eye. The relationship shows a rather flat region between  $-10$  pN and  $1$  pN. In that region, the velocity as a function of ATP concentration follows a Michaelis-Menten-like relation. This region is followed by an abrupt drop between  $1$  pN and  $2$  pN. Above the stall force, the motor is pulled backwards with a velocity that increases roughly linearly with load and is independent of the ATP and ADP concentration.

## Five models for myosin V

Baker et al. (30) measure values around 1  $\mu\text{m}$ , while the data of Clemen et al. (14) are closer to 300nm. A possible explanation for this apparent discrepancy could lie in the fact that actin filaments were attached to the glass surface in the latter experiment, which possibly hindered the motor in its natural helical motion around the filament and caused a premature dissociation. Therefore, one can accept run length values around 2  $\mu\text{m}$  for unconstrained motion along actin filaments.

The mean run length over a wide range of nucleotide concentrations, but without an applied load, has been measured by Baker et al. (30). It shows a slight decrease with a growing ATP concentration. Added ADP decreases the run length, but only by about a factor of 2, which is reached at concentrations around 200  $\mu\text{M}$ . Under higher ADP concentrations, the run length remains constant at around 400nm. Added 40 mM phosphate led to a reduced run length (30) at zero load and to a lower load at which the molecule dissociates (54).

Knowledge on the load-dependence of the run length is still rather incomplete. Clemen et al. (14) measure a largely constant run length of about 300nm under loads ranging between -5pN and 1.5pN. Under a super-stall load of 5pN, the average backward run length was 80nm.

The run length decreases with an increasing ionic strength (30,55). It could be increased by adding (through mutation) additional positive charge to loop 2, which increases the electrostatic attraction between the myosin V head and actin (55).

### 3.5. Kinetics

These mechanical data are directly complemented by *kinetic measurements*, which follow the transitions that take place when motor molecules with a certain nucleotide (ATP or ADP) are mixed with actin filaments and a different nucleotide in solution. There are generally two ways of probing the myosin V kinetics - using single-headed (usually S1) molecules, or double-headed motors. Experiments on single-headed motors reveal the kinetics of the unstrained ATPase cycle. Experiments with double-headed motors, on the other hand, bring additional insight into the kinetics in states where both heads are bound and some transitions are suppressed (or possibly in some cases accelerated) by intra-molecular strain.

#### 3.5.1. Single-headed

Kinetic studies on single-headed myosin V molecules were pioneered by De La Cruz and coworkers. In Refs. (17,20), a number of kinetic rates have been determined. These include the ATP binding rate (both in free heads and on actin), the ATP hydrolysis rate, the phosphate release rate on actin, the ADP release and re-binding rate (in free/bound heads), and the actin-myosin binding/unbinding rate in apo (state without any nucleotide) and ADP states. Trybus et al. (56) report similar values, but with a large discrepancy with regard to the ADP release rate in free heads. Wang et al. (57), on the other hand, report a slower phosphate release rate. Forgacs

et al. (58) measured the kinetics with deac-aminoATP. In summary, one can say that the kinetics of single-headed myosin V is well characterised, except for some short-lived states (such as the dissociation rate in the ATP state) or rare transitions (such as dissociation in the ADP.Pi state).

#### 3.5.2. Double-headed

Kinetic measurements on double-headed myosin V molecules in the presence of actin are crucial for a quantitative understanding processive motility and the coordination of chemical cycles. At the same time, they are much more difficult to interpret, because one measures a superposition of contributions from the lead head, from the trail head and from molecules bound with a single head only.

The first kinetic study on dimers was carried out by Rosenfeld and Sweeney (59). They found that myosin V with ADP, mixed with actin, binds with both heads and releases ADP from the trail head at a rate of 28-30s<sup>-1</sup> and from the lead head at about 0.3-0.4s<sup>-1</sup>. Note that the ADP release rate from the trail head is somewhat (by about a factor of 2) accelerated in comparison with single-headed myosin V, while it is strongly suppressed on the lead head. This is attributed to the effect of intra-molecular strain, which affects the ATP release both from the lead and from the trail head. If myosin V with ADP and Pi on it is mixed with actin, it releases phosphate from both heads at a measured rate of about 200s<sup>-1</sup>. However, obtaining this rate involved some extrapolation, so the lower values obtained in later studies (60,61) might be more reliable. But the important message of the paper is that the lead head releases phosphate quickly and then waits in the ADP state. ADP release from the lead head was therefore identified as the key gating step in the chemical cycle.

As a result of these kinetic studies, the duty cycle shown in Figure 3 has emerged with a high level of consensus.

## 4. OPEN QUESTIONS

Yet some of the important questions on myosin V have only been partially answered so far. In the following, we will discuss five major open questions. They are, on one side, important for setting up theoretical models. At the same time, most of these questions are quantitative in nature and most of them concern properties that are not directly observable in an experiment. Therefore, they can only be tackled efficiently by combining experimental results with theoretical models.

### 4.1. Head-head coordination

In order to maintain its processivity, a dimeric motor has to prevent simultaneous detachment of both heads from its track. This means that the chemical cycles of both heads have to be coordinated in order to stay out of phase. There is a high level of agreement that this coordination is achieved through intra-molecular strain. There is also undisputed evidence for *lead head gating*, which means that ADP release from the lead head waits until the trail head detaches from actin (59,61,62).

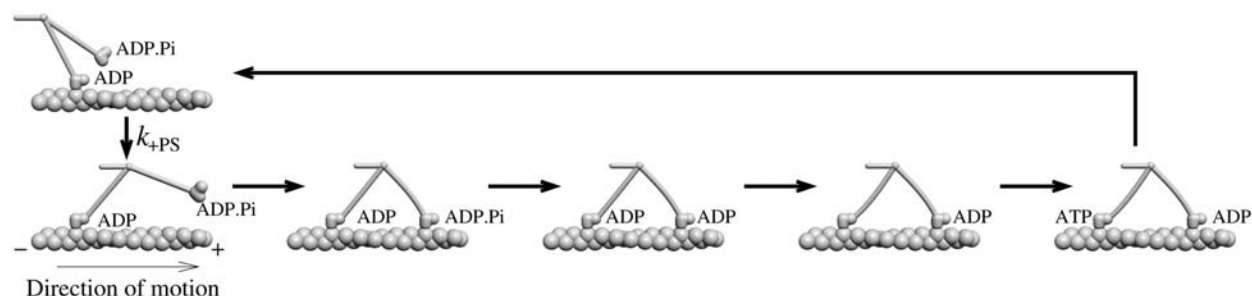


**Figure 3.** Duty cycle of a dimeric myosin V motor. A head with ADP undergoes the power-stroke, then the second head containing ADP.Pi binds in the lead position, it releases Pi, then the rear head releases ADP, binds a new ATP molecule and detaches from actin. After that the cycle repeats with exchanged roles of the two heads and with the motor one step further.

However, there is also some evidence for much weaker gating in the trail head, meaning that the ADP release rate in the trail head is somewhat accelerated by the presence of the bound lead head (12,59).

Both effects are likely connected with the small (about 5 nm for single-headed molecules) conformational change that takes place upon ADP release (12,63). Conversely, Oguchi *et al.* (64) have recently directly measured the influence of an applied load on the ADP binding affinity. The strong deceleration of ADP release in the lead head is possibly also connected with the large main power stroke. The exact nature of this influence depends on whether the “telemark state” exists or not (see next section).

In addition, coordination can take place during other steps, too. The elastic lever arm model shows that the attachment rate of the lead head is strongly suppressed before the trail head goes through a power-stroke (45).

#### 4.2. Lead head state

One of the most controversial questions on myosin V is whether the lead head is in the pre-powerstroke state, or in the post-powerstroke state with a strongly bent lever arm (also called “telemark” state, because the shape of the molecule resembles a telemark skier with the front knee bent), as shown in Figure 4. Evidence for the telemark state first came from EM images (24), although subsequent analysis revealed that molecules with a kinked leading lever arm are not as abundant as those with a straight one (25), and that the telemark state might not lie on the main pathway. Further evidence came from experiments with fluorescence polarisation (22,65), which showed that about a third of labels attached on the lever arm did not show any detectable tilting motion. But later studies revealed that this was probably a consequence of the ambiguity in angle detection from one vector component alone and that all labels on the lever arm do indeed show tilting motion, as well as alternating steps (66,67).

However, it is still possible that the head domain of the lead head is in some intermediate state and that its

lever arm is bent, but not as strongly as in the pure telemark state.

#### 4.3. Sub-steps

An intriguing question is whether the motor moves its load in uniform steps, or do they contain short-lived substeps. Because of the noise in position determination, these sub-steps are difficult to detect. The experiment of Uemura and co-workers (16) revealed substeps of 11nm+24nm, as shown in Figure 5A. Their length was independent of load, but their duration was increased both with an increasing load and upon addition of BDM (butanedione monoxide). The duration was independent of the ADP and ATP concentration.

The second important observation related to sub-steps comes from Cappello *et al.* (52). This study employs travelling wave tracking, a technique that allows a significantly higher temporal resolution. It reveals two substeps of about 5nm: one immediately preceding and one immediately following the main step (Figure 5B). The duration of the substep before the main step was longer at a lower ATP concentration. Therefore, neither of the two sub-steps has a direct correspondence in the observation of Uemura *et al.* The substep following the main step can well be attributed to the diffusive search of the lead head for the next actin binding site. The explanation for the step preceding the main step is more difficult. The authors propose a hypothesis in which the substep represents a reversible transition in the lead head that can take place after the trail head releases ADP and which is a necessary condition for ATP binding to the trail head. One question that remains open in this scenario is the mechanism by which ATP binding to the trail head could be triggered by a transition in the lead head.

Sub-steps have also been observed in two somewhat different experiments. First, Dunn and Spudich (49) have labelled sites on the lever-arm with gold nanoparticles and tracked it with sub-millisecond time resolution. They found that the 74 nm steps were subdivided into 49 nm+25 nm and that the intermediate state had a very high level of fluctuations, resulting from

## Five models for myosin V



**Figure 4.** In the model without a telemark state (left), the lead head stays in the pre-powerstroke state before the trail head detaches. In the telemark state (right), both heads are in the post-powerstroke state, but the leading lever arm has a strong kink – resembling a telemark skier.

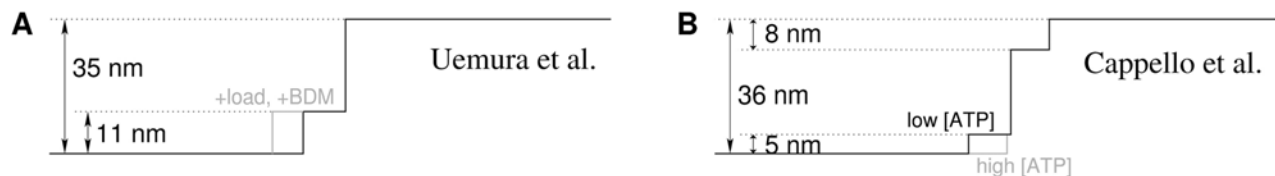


**Figure 5.** Sub-steps as observed by Uemura *et al.* (A) and Cappello *et al.* (B). Uemura *et al.* observe a substep of 11 nm, preceding the main step. Its size is independent of load, but its duration increases with load or upon addition of BDM. Cappello *et al.* observe one substep preceding the main step (only at low ATP concentrations) and one following the main step (independent of ATP concentration).

the free head diffusively searching for the next binding site. Depending on the light chain presence, the lead head binding rate was either or . It was slowed down by the presence of BDM – different from the conclusion of Uemura *et al.* (16) that the effect of BDM is a delayed power stroke. The lead head binding rate is somewhat slower (possibly because of the attached particle), but still of the same order of magnitude as the duration of the second sub-step (1-2 ms) measured by Cappello *et al.* (52). A direct comparison of step sizes between the two experiments is difficult, because Cappello *et al.* tracked the cargo position, whereas Dunn and Spudich tracked a bead attached to the lever arm.

Finally, as already mentioned, a sub-step of about 5 nm has been observed by Veigel *et al.* (12,63) in single-headed myosin V molecules and identified as the conformational change upon ADP release. There are good reasons to believe that this sub-step is not directly observable in dimeric motors (45). One argument is that ADP release shows a strong load dependence in single-headed motors (63,64). In dimeric motors, moderate backward loads up to ~1 pN or forward loads show almost no effect on the stepping rate, which is (under saturating ADP concentrations) limited by ADP release (4,16). However, Cappello *et al.* hypothesise that the conformational change upon ADP release in the trail

head might be involved in triggering a reversible transition in the lead head, which then causes an observable sub-step (52).

### 4.4. How tight is the coupling between the hydrolysis cycle and the stepping?

The Michaelis-Menten like dependence of the kinesin velocity on the ATP concentration (68) was seen as early evidence for a tight coupling between ATP hydrolysis and stepping (in fact, those experiments could not yet exclude additional futile ATP hydrolysis cycles). Similar experiments also revealed tight coupling between stepping and ATP hydrolysis in myosin V under low loads (10). Therefore, early kinetic models assumed ATPase cycles tightly coupled to the stepping (44,69), which means that the motor always makes one step when it hydrolyses one ATP molecule and that it can only make a backward step upon re-synthesis of an ATP molecule from ADP and phosphate.

Such reversible behaviour has indeed been demonstrated in the  $F_1$ -ATPase, which can either hydrolyse or synthesise ATP, depending on the direction of rotation (70). However, experiments on both myosin V and kinesin have shown that tight coupling has its limits under high loads. For kinesin, Carter and Cross (71) found out that under high loads the motor is pulled

## Five models for myosin V

backwards, for which it requires ATP binding. The observation that myosin V can be pulled backwards by a super-stall force was first made by Clemen and coworkers (14). The backward and forward steps were further investigated in a subsequent paper (15), where they found out that forward steps involve ATP hydrolysis, while backward steps involve neither hydrolysis nor synthesis of ATP. A rather surprising consequence of this finding is that a high load (e.g., 5pN) can pull the motor faster when applied in the backward direction than in forward.

So under sufficiently high loads, both myosin V and kinesin leave the tightly coupled cycle, but each in a different way: kinesin can be pulled backwards in the presence of ATP, whereas myosin V does not require it.

### 4.5. Source of elasticity

In any mechano-chemical model for myosin V, there needs to be at least one elastic element, such as the lever arm. One reason is that some degree of flexibility is necessary in order for the motor to be able to bind to the actin filament with both heads simultaneously. Furthermore, many models propose that when a head commits its power stroke, some of the free energy released is first stored into elastic energy and later uses it to perform work on the load. Besides the lever arm, which could be an obvious elastic element, further candidates for the source of compliance lie in or around the converter domain. In particular, the converter domain was shown to be the main source of compliance in myosin II (72). However, the same study showed that the converter domain was significantly stiffened through a single mutation, which means that the result is not directly transferable between different myosin classes.

Measuring the stiffness directly requires careful elimination of other sources of compliance, such as the actin filament and the tail domain. Veigel *et al.* measured the stiffness of single-headed myosin V and obtained the value 0.2pN/nm (63). A comparison with smooth muscle myosin led to the suggestion that the elastic element is located close to the pivot point of the lever arm. Of course, this conclusion cannot be regarded as definite, because the degree of mechanical similarity between the two types of myosin is not known.

On the other hand, the existence of a telemark state would suggest that the lever arm has a very compliant point (sufficiently compliant that it can be bent by the power-stroke). MD simulations (73) support the possibility of such a kink, but are not yet capable of predicting the bending energy connected with it.

## 5. THEORETICAL MODELS

### 5.1. Overview

Theoretical models can be employed to describe the dynamics of a motor protein on different levels. First, there are discrete stochastic models that describe the motor with a collection of chemical states that correspond to different positions along the track

(75). The motor protein is treated as a “black box”, the only observable being the tail- or the cargo position. This approach is particularly useful for interpreting experimental results gained with optical tweezers, such as force-velocity relations under different ATP, ADP and phosphate concentrations. It was first applied to myosin V by Kolomeisky and Fisher (44). The basic version of a discrete stochastic model allows no events beyond the regular chemical cycle, but it can be extended to allow parallel pathways (47,48,76), as well as dissociation from the actin filament. Coordinated hand-over-hand motility is one of the assumptions of such models, rather than being its outcome.

The next level of models uses a similar phenomenological approach to describe each individual head. The properties of a dimeric motor are then derived from those of the two heads. This approach is similar to that taken by muscle myosin models (77-79), which deal with a large number of myosin heads, assembled into thick filaments. Such models combine the head domain, described with a few discrete chemical states, with an elastic element that connects it to the other head and to the tail. We will therefore use the term *mechano-chemical models* for this category. Two models for myosin V that follow this approach are described in Refs. (45) and (46). In theory, the mechano-chemical models can be mapped onto corresponding discrete stochastic models. A state in the resulting discrete stochastic model is then described with a combination of the lead head state, the trail head state and the relative distance of the two heads on the track. Without further simplifications, the number of such states is therefore usually too high to be studied analytically.

Finally, there are molecular models for motor proteins that attempt to understand the mechanism of energy transduction in microscopic detail. A full scale molecular dynamics simulation over millisecond time scales on which the chemical cycle takes place is still well beyond the available computational power, but it can be used to probe essential processes in the course of ATP hydrolysis (80-82). Also, several approximative methods have been employed. The dynamics of the power stroke has been investigated with molecular kinematics using the minimum energy path method (MEP) (83,84). While these computational models represent an important contribution to our understanding of the microscopic mechanism by which molecular motors work, they are currently not yet precise enough to make predictions on free energy differences between different states or transition rates between them. Therefore, quantitative models still need to be “reverse-engineered” to a large extent from experimental data.

There are other noteworthy models that deal with special aspect of myosin V, but will not be the subject of our review. Here we should briefly mention the work of Smith, which relates the duty ratio of myosin V to its processivity (85). Further, there is a study by Schilstra and Martin (86) who investigate how viscous load can decrease

**Table 1.** Comparison of five theoretical (kinetic and mechano-chemical) models

	Kolomeisky (44)	Skau (47)	Wu (48)	Lan (46)	Vilfan (5-st.) (45)
<b>Force-velocity relation:</b>					
Flat region around zero force	○	○	n/a	+	+
Flat for high forward loads	–	+	n/a	○	+
Around stall	+	+	n/a	+	+
Above stall	○1	–	n/a	○2,3	○4
[ATP] dependence	+	+	+	n/a	+
[ADP] dependence	n/a	+	+	n/a	+
<b>Substeps:</b>					
As observed by Uemura (16) (11nm+24nm, load independent)	+	–	+	?6	–
As observed by Cappello (52), before main step (only at low [ATP])	–	–	–5	?6	–7
As observed by Cappello (52), after main step	–	+	–	?6	+
<b>Processivity (run length):</b>					
[ATP] dependence at zero load	n/a	+	○	n/a	+
[ADP] dependence at zero load	n/a	–	+	n/a	○
Load dependence: super-stall forces	n/a	–	n/a	n/a	+
Load dependence: forward forces	n/a	+	n/a	n/a	○8

“+” denotes that the given experimental observation is in agreement with the model. “○” means partial or qualitative agreement, “–” denotes disagreement, “n/a” (not applicable) that the given aspect is not included in the model or that no analysis is available that would allow a comparison. <sup>1</sup>Model shows backward stepping, but only through ATP synthesis <sup>2</sup>Velocity too high; dependence on ATP concentration not available. <sup>3</sup>In the refined model (74) no backward stepping takes place above 3pN load. <sup>4</sup>Velocity too low. <sup>5</sup>Model shows a substep upon trail head release, but predicts an incidence that increases with the ATP concentration. <sup>6</sup>Histograms of position changes show intermediate peaks, but no analysis is available which would attribute them to any type of sub-steps. <sup>7</sup>Model shows a substep upon trail head release, but it does not depend on ATP concentration. <sup>8</sup>Model processive only up to 3pN forward load.

the randomness of the walking molecule. Finally, a number of models deal with the collective dynamics of motors in general (87,88), and those findings could be relevant for the dynamics of myosin V transporting vesicles, too.

In the following, we will give an overview over 3 discrete stochastic models and 2 mechanochemical ones. In particular, we will identify the common points and the differences between them. Table 1 shows an overview which model properties are in agreement with which experimental results and where the discrepancies are.

## 5.2. Discrete stochastic models

### 5.2.1. Kolomeisky and Fisher

Kolomeisky and Fisher (44) (Figure 6A) presented the first theoretical model describing myosin V. It uses 2 states per step. The intermediate state corresponds to a substep of about 13nm, measured from the ATP binding state. The model parameters were determined by fitting the calculated force-velocity relations to data from Ref. (4). The conclusions of the study are that both the ATP binding rate is load-independent and the ADP release rate is only weakly load dependent – which implies that most of the load dependence is contained in their reverse rates. At super-stall forces, the model shows backward steps, but they require ATP synthesis. Besides fitting the load velocity relations, the model also makes predictions on the randomness parameter of the trajectory (89), defined as

$$r = \lim_{t \rightarrow \infty} \frac{\langle x^2(t) \rangle - \langle x(t) \rangle^2}{a \langle x(t) \rangle}, \quad (1)$$

where  $a$  denotes the step size and  $\langle \dots \rangle$  an ensemble average. The value of  $r$  is 1 for a stepper with a single rate

limiting step. A higher value of indicates the presence of backward- or multiple steps, while  $r < 1$  means that several rate limiting transitions per step are involved. For myosin V, the randomness parameter has not yet been measured to date.

Prediction of substeps of a similar size as later observed by Uemura *et al.* (16) is a particular merit of this model. However, it should be mentioned that the observed substeps had a duration around 10ms. In the model, the duration of substeps corresponds to the ADP release time, which is around 80ms. This discrepancy is an indication that two states per step are not sufficient if one wants to describe the myosin V motion in this amount of detail.

### 5.2.2. Skau, Hoyle and Turner

Skau *et al.* (47) (Figure 6B) developed a more elaborated myosin V model, which still belongs to the category of discrete stochastic models, but includes two parallel cycles - one that leads to a forward step and a futile one that does not. In addition, one dissociation path from actin is included. The model does not include backward stepping without ATP synthesis. Substeps of 25+11nm are included in the model, but in reverse order compared with the model by Kolomeisky and Fisher (44) and the experimental observation by Uemura *et al.* (16), where ATP binding is followed first by a short (12nm) and then the longer (24nm) substep, rather than the long step followed by the short one.

The model fits well the force-velocity relations, although the velocity starts to drop around zero force already, rather than being nearly flat up to about 1pN, as experimental data suggest. Because the model does not include backward stepping by other means than reversing the ATP hydrolysis, it fails to reproduce the velocity at super-stall loads.



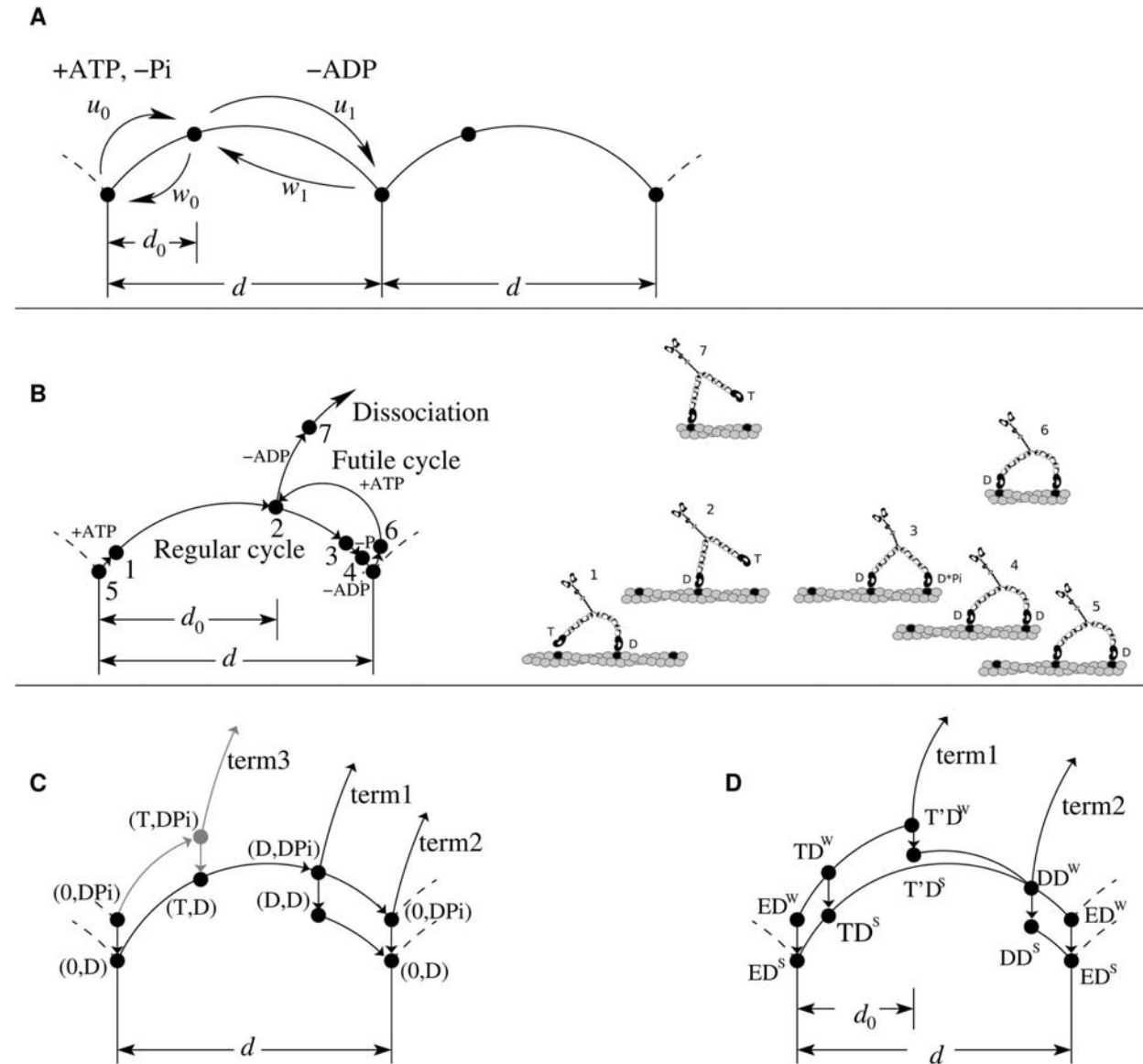


**Figure 6.** 4 kinetic models with different levels of complexity. (A) Model by Kolomeisky and Fisher (44) (B) Model by Skau, Hoyle and Turner (47). The right part shows the states numbered 1-7. Note that states 1,3,4,5 and 6 have the same load position. (C) Model by Baker *et al.* (30) (D) Model by Wu, Gao and Karplus (48).

The calculated run length increases inversely proportional with a decreasing ATP concentration. It also increases with an increased ADP concentration – the latter is inconsistent with the measurement of Baker *et al.* (30).

### 5.2.3. Wu, Gao and Karplus

Wu *et al.* (48) (Figure 6D) recently proposed a model that contains more kinetic details, but no external force (load). In that model, each head can be found in the empty state, in the ATP state, in the detached ATP state, in the weakly bound ADP state and in the strongly bound ATP state. The trail head can either be in the empty, ATP, or strongly bound ADP state. The lead head can be in the strongly or weakly bound ADP state. The chemical cycle can follow three different pathways (mainly depending on

when the weakly- to strongly-bound transition in the leading head takes place). Upon trail head detachment, the tail moves by 12nm, corresponding to the substep from Ref. (16). This substep occurs only on one of the three kinetic pathways, which is in agreement with the experiment that showed substeps only for a fraction of steps. There are also two different termination pathways, which lead to the dissociation of the whole dimer from actin.

The main results of the model are zero-load velocity and run length as a function of ATP and ADP concentration. The calculated run length shows a decrease with the ADP concentration, which is in good qualitative agreement with Ref. (30). The run length increases

## Five models for myosin V

somewhat with an increasing ATP concentration, which is different from the conclusion of Baker and coworkers (30), although, given the uncertainty of data points, not necessarily inconsistent with their measurements. The model shows that the velocity at low ATP concentrations is very sensitive to ADP, which could possibly provide a reconciliation of the large differences between different experimental results.

A question that is beyond the scope of a purely kinetic model, but will have to be answered when mechanical aspects are included, is how the intra-molecular strain can have such a strong influence on the weakly- to strongly-bound transition in the lead head. In the model, the transition rate decreases almost 4-fold when the trail head releases ADP. Another puzzle brought up by the model is why the dissociation rate is 30 times higher in a state where both heads are bound to actin (one weakly and one strongly) than in a state where only one head is weakly bound to actin and the other one is free. While this seems inevitable for an explanation of run length data by Baker *et al.* (30), it is not easy to think of a mechanical model in which myosin V, bound with both heads, is more likely to dissociate than when bound with a single head. Internal strain might potentially provide an explanation, but only if the dissociation takes place in a single step and not with one head after the other.

### 5.3. Mechano-chemical models

The main difference between the models listed above and the mechano-chemical approach is that the latter uses a *single myosin V head* as the model unit and derives the properties of a dimer. This reduces the number of parameters and model assumptions. The model is specified by the states of an individual head (typically 4 or 5 bound states, plus a number of free states), by the mechanical conformation of the molecule in that state, by the transition kinetics and by the interaction between the two heads that is mediated by the mechanical properties of the lever arms joining them. In practice, however, even the kinetics of a single head contains a number rates that have not yet been measured directly and that need to be determined from dimer properties, such as force-velocity relation and processivity. So far, two myosin V models have been developed on these premises: the model by Lan and Sun (46) and the elastic lever arm model (45). Although they share the basic principle, there are significant differences in the implementation.

#### 5.3.1. Lan and Sun

Lan and Sun (46) proposed a model based on a cycle with 5 chemical states, all of which can in theory be bound to actin or free. The transition rates are taken from kinetic studies or guessed on the basis of other myosins where no data are available. Nonetheless, some assumed rate constants differ significantly from generally accepted values. For instance, the detachment rate of a head from actin in the empty state is assumed to be  $0.16 \text{ s}^{-1}$ , while the value from Ref. (17) is  $0.00036 \text{ s}^{-1}$ .

The elasticity of the two lever arms is modelled as highly anisotropic. It combines an in-plane component

and a very stiff azimuthal component. The in-plane elasticity corresponds to a persistence length of 120nm, or a spring constant of 0.05 pN/nm, measured at the tip. This is consistent with an earlier estimate based on tropomyosin (90), but much lower than the stiffness measured with optical tweezers (0.2 pN/nm (63)). The azimuthal component is modelled in an *ad hoc* way and is assumed to be very stiff. If the model molecule binds to two adjacent sites on the actin filament, the bending energy is  $40 k_B T$ , compared to  $15 k_B T$  in the model with isotropic lever arm elasticity (45).

In contrast with the model in Ref. (45), the heads also possess internal flexibility, meaning that the lever arm angle can fluctuate to some extent while the head stays in the same chemical state. This allows the transitions to take place without the need for a simultaneous lever arm swing.

The main result of the model is the force-velocity relation for a fixed set of nucleotide concentrations. It reproduces well the flat region at low loads and the abrupt drop around 1pN, but there is a discrepancy above the stall force, where it predicts a backward speed well above experimental values. No processivity calculations are made in the paper, so it is likely that the parameters will need adjustment to achieve realistic run lengths.

A subsequent paper by the same authors (74) deals primarily with myosin VI, but it also presents a refined model for myosin V. This includes a simpler kinetic model, described with a 4-state cycle. The second important change is that the lever arm elasticity is modelled in a more realistic way, as an anisotropic elastic beam with persistence length values of 150 nm and 400 nm in two different planes. The elastic energy in a state where the two heads are separated by two actin subunits is reduced to about  $10 k_B T$ , as compared with  $40 k_B T$  in the original model. The calculated force-velocity relation remains similar as in the older model for forward and below-stall loads. For super-stall forces, the new model predicts nearly negligible backward velocities.

#### 5.3.2. Elastic lever arm model

The elastic lever arm model (45) arose from a similar concept, but has many differences in the implementation. The paper presents two alternative chemical cycles: the 4-state and the 5-state cycle. The 5-state cycle allows phosphate release from the lead head before the power-stroke, while the 4-state cycle does not. Note that model calculations and also later experimental evidence strongly favour the 5-state scenario, so we will focus our discussion of the model on it. The model uses a cycle of 4 attached and one detached state (plus the detached ADP state, which is not part of the regular cycle). Some short lived states (e.g., bound with ATP) are omitted, as are some improbable ones (e.g., unbound head in the empty state).

The lever arm is modelled as an isotropic elastic beam with a bending modulus of 1500 pN/nm, which corresponds to a persistence length of 360 nm, or a spring constant of 0.25 pN/nm measured at the lever arm tip. Both

## Five models for myosin V

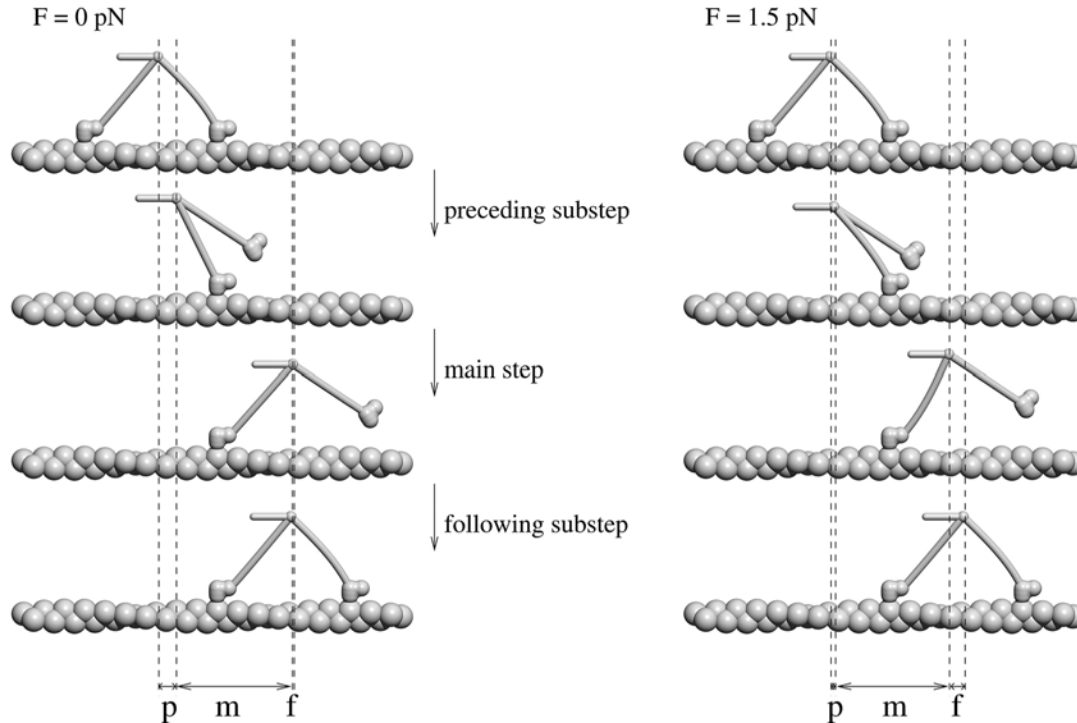


**Figure 7.** Substeps in the elastic lever arm model. Because they involve changes between configurations bound with a single and with both heads, their size depends on load.

lever arms are connected with a fully flexible joint (the validity of this assumption was recently proven by Dunn and Spudich (49)).

Based on the above value for the elasticity of the lever arm we estimated that the lead head cannot commit its power-stroke before the trail head detaches, meaning that the telemark state does not occur. However, we cannot fully exclude that nonlinearities in the elastic properties of the lever arm still sometimes allow this configuration.

The fact that ADP release takes place in the trail head while the lead head is attached to actin provides a direct explanation for the flat force-velocity curve below 1 pN load. Namely, although the ADP release is connected with a small conformational change in the trail head, it causes virtually no load movement. Conversely, the load therefore has no influence on the ADP release rate, which in turn determines the velocity. For higher loads, close to stall, other transitions (power stroke or lead head binding) become rate limiting and the velocity then drops abruptly.

The model reproduces well the force-velocity relation up to the stall load. For super-stall forces, the model predicted backward slippage without ATP hydrolysis. It occurs when both heads have ADP on them. Very similar behaviour was later discovered by Gebhardt and coworkers (15). However, the backward sliding speed in the model is too low. Another discrepancy is that experimentalists observe backward slippage even in the absence of any nucleotide, while the model needs at least

ADP in order to move backwards. This is due to the assumption that the detachment rate of a head with ADP or with no nucleotide is the same for the lead and the trail head, and that it is independent of strain. In order to quantitatively fit the newer data, a strain-dependent detachment rate in empty and ADP states will therefore be necessary.

The model shows a short substep preceding the main step, which is connected with the trail head detachment. It also shows a sub-step following the main step, which corresponds to the binding of the lead head. The second substep is in good agreement with the observation of Cappello *et al.* (52). The first substep is not fully compatible with their experimental result, because it shows no dependence on the ATP concentration. In total, one can still say that the substeps from that model are much closer to the experimental results of Cappello *et al.* (52) than to those of Uemura *et al.* (16). In both intermediate states before and after the main steps the motor is bound with a single head and therefore has a much higher compliance. Therefore, both substep sizes depend on the load. The first substep decreases with load (Figure 7), while the second increases. Uemura *et al.* (16), on the other hand, see load-independent substep sizes.

Another major advantage of the mechano-chemical approach is that dissociation events that limit the run length are an inevitable and integral part of the model and do not need any additional assumptions or parameters. However, they do depend on several of the kinetic

**Table 2.** Dissociation pathway “dictionary”

Pre-dissociation state (trail,lead)	Vilfan (45)	Baker <i>et al.</i> (30)	Wu <i>et al.</i> (48)	Skau <i>et al.</i> (47)
(A.M.T, A.M.D.Pi <sup>1</sup> )	Path 1	Term3 (excluded)	term1	-
(A.M.T, M.D.Pi)	Path 2		-	Termination (sole pathway)
(A.M.D, M.D.Pi) (A.M.D, M.D <sup>1</sup> )	Path 3	term1	term2	-
(A.M, A.M.D.Pi)	-	term2	-	-

The first column denotes the state of the dimer from which dissociation occurs. For example (A.M.T,A.M.D.Pi) means that the trail head is bound to actin with ATP on it, while the lead head is bound to actin with ADP and Pi. The other columns show the names of these dissociation pathways in different models. Evidence exists that “Path 3” is the predominant dissociation path.

<sup>1</sup>weakly bound A.M.D in (48)

constants whose values are not yet well known to date. The model shows that there are generally 3 classes of dissociation pathways.

Note that different models in the literature use quite different terminology for dissociation pathways. They are not entirely one-to-one translatable, mainly because the models of Baker (30) and Wu (48) include weakly bound lead head states with ADP.Pi and ADP on them, respectively. Other models do not distinguish between weakly and strongly bound states. So Table 2 presents the best effort of a “dictionary”, showing equivalent dissociation (termination) pathways in four models that include dissociation events.

With the parameters used in the original paper, the model reproduces realistic run lengths for zero load. It also shows a run length that falls with ATP for concentrations above 50  $\mu$ M. The run length decreases with an increasing ADP concentration - however, the findings of Baker *et al.* (30) are only partially reproduced. A more serious discrepancy is that the dissociation rate becomes very high for strong forward loads. Newer experiments have shown that myosin V stays attached to actin for a few seconds even under 10pN forward load (15). Therefore, dissociation pathways 1 and 2 are likely overestimated in Ref. (45).

The model was later expanded to take into account torsional fluctuations in the actin structure, which lead to an improved agreement between the calculated and the measured step size distribution (91). It was also used to calculate the behaviour of myosin V when it encounters an Arp2/3 mediated filament branch (92). The predicted branching probability is in good agreement with data by Ali *et al.* (93).

## 6. CONCLUSIONS

Our comparison has shown that there is no myosin V model so far that would fit *all* available experimental data. A particular problem is to explain the high processivity over a wide range of loads. Additionally, our experimental knowledge about processivity is still somewhat incomplete. Data on load dependence of the run length for different ATP and ADP concentrations would be immensely useful. However, a glance at Table 2 possibly reveals the lines of a future consensus on the dissociation

mechanism. Baker *et al.* (30) conclude that “term1” is the predominant dissociation pathway. In the elastic lever arm model (45), three pathways are present, but only Path 3 shows a dependence that allows a high degree of processivity for forward loads. Wu *et al.* (48) consider two pathways, but use a higher dissociation rate for “term2”. These terms all denote more or less the same dissociation pathway, namely dissociation from the waiting, (A.M.ADP,A.M.ADP) state. The model by Skau *et al.* (47), however, uses a completely different path. The consequence is that the run length strongly decreases with load, so that the model motor loses processivity when the load approaches 1pN.

With regard to sub-steps, there is still some discrepancy among experimental results (16,52). This controversy will have to be sorted out. In addition, more data on load- and nucleotide dependence of the substep size and duration will provide valuable input for future theoretical models.

Finally, let us remark that all theoretical models described here are largely phenomenological. Connecting them in a quantitative manner with our knowledge of the conformational changes that take place inside the myosin head, such as opening/closing of switch 1, switch 2 and the cleft (27,60,94-98), remains a major challenge for the future.

## 7. ACKNOWLEDGMENTS

I would like to thank Martin Karplus and Anatoly Kolomeisky for helpful comments on the manuscript. This work was supported by the Slovenian Research Agency (Grant P1-0099).

## 8. REFERENCES

1. Kieke M. C., M. A. Titus: The myosin superfamily: An overview. In: *Molecular Motors*. Ed: Schliwa M., Chaper 1, 3-44, Wiley-VCH, Weinheim, Germany (2003)
2. Reck-Peterson S. L., D. W. Provance, Jr., M. S. Mooseker, J. A. Mercer: Class V myosins. *Biochim Biophys Acta* 1496, 36-51 (2000)
3. Langford G. M.: Myosin-V, a versatile motor for short-range vesicle transport. *Traffic* 3, 859-865 (2002)

## Five models for myosin V

4. Mehta A. D., R. S. Rock, M. Rief, J. A. Spudich, M. S. Mooseker, R. E. Cheney: Myosin-V is a processive actin-based motor. *Nature* 400, 590-593 (1999)
5. Rock R. S., S. E. Rice, A. L. Wells, T. J. Purcell, J. A. Spudich, H. L. Sweeney: Myosin VI is a processive motor with a large step size. *Proc Natl Acad Sci USA* 98, 13655-13659 (2001)
6. Yang Y., M. Kovacs, T. Sakamoto, F. Zhang, D. P. Kiehart, J. R. Sellers: Dimerized Drosophila myosin VIIa: a processive motor. *Proc Natl Acad Sci USA* 103, 5746-5751 (2006)
7. Tominaga M., H. Kojima, E. Yokota, H. Orii, R. Nakamori, E. Katayama, M. Anson, T. Shimmen, K. Oiwa: Higher plant myosin XI moves processively on actin with 35 nm steps at high velocity. *EMBO J* 22, 1263-1272 (2003)
8. Rock R. S.: Navigating the cytoskeleton with myosin X. *Biophys J* 94, Part 2, Suppl. S, abstract 62-Symp (2008)
9. Post P. L., M. J. Tyska, C. B. O'Connell, K. Johung, A. Hayward, M. S. Mooseker: Myosin-IXb is a single-headed and processive motor. *J Biol Chem* 277, 11679-11683 (2002)
10. Rock R. S., M. Rief, A. D. Mehta, J. A. Spudich: *In vitro* assays of processive myosin motors. *Methods* 22, 373-381 (2000)
11. Rief M., R. S. Rock, A. D. Mehta, M. S. Mooseker, R. E. Cheney, J. A. Spudich: Myosin-V stepping kinetics: a molecular model for processivity. *Proc Natl Acad Sci USA* 97, 9482-9486 (2000)
12. Veigel C., F. Wang, M. L. Bartoo, J. R. Sellers, J. E. Molloy: The gated gait of the processive molecular motor, myosin V. *Nat Cell Biol* 4, 59-65 (2002)
13. Purcell T. J., C. Morris, J. A. Spudich, H. L. Sweeney: Role of the lever arm in the processive stepping of myosin V. *Proc Natl Acad Sci USA* 99, 14159-14164 (2002)
14. Clemen A. E., M. Vilfan, J. Jaud, J. Zhang, M. Barmann, M. Rief: Force-dependent stepping kinetics of myosin-V. *Biophys J* 88, 4402-4410 (2005)
15. Gebhardt J. C., A. E. Clemen, J. Jaud, M. Rief: Myosin-V is a mechanical ratchet. *Proc Natl Acad Sci USA* 103, 8680-8685 (2006)
16. Uemura S., H. Higuchi, A. O. Olivares, E. M. De La Cruz, S. Ishiwata: Mechanochemical coupling of two substeps in a single myosin V motor. *Nat Struct Mol Biol* 11, 877-883 (2004)
17. De La Cruz E. M., A. L. Wells, S. S. Rosenfeld, E. M. Ostap, H. L. Sweeney: The kinetic mechanism of myosin V. *Proc Natl Acad Sci USA* 96, 13726-13731 (1999)
18. De La Cruz E. M., A. L. Wells, H. L. Sweeney, E. M. Ostap: Actin and light chain isoform dependence of myosin V kinetics. *Biochemistry* 39, 14196-14202 (2000)
19. De La Cruz E. M., H. L. Sweeney, E. M. Ostap: ADP inhibition of myosin V ATPase activity. *Biophys J* 79, 1524-1529 (2000)
20. Yengo C. M., E. M. De la Cruz, D. Safer, E. M. Ostap, H. L. Sweeney: Kinetic characterization of the weak binding states of myosin V. *Biochemistry* 41, 8508-8517 (2002)
21. Ali M. Y., S. Uemura, K. Adachi, H. Itoh, K. Kinoshita, Jr, S. Ishiwata: Myosin V is a left-handed spiral motor on the right-handed actin helix. *Nat Struct Biol* 9, 464-467 (2002)
22. Forkey J. N., M. E. Quinlan, M. A. Shaw, J. E. Corrie, Y. E. Goldman: Three-dimensional structural dynamics of myosin V by single-molecule fluorescence polarization. *Nature* 422, 399-404 (2003)
23. Yildiz A., J. N. Forkey, S. A. McKinney, T. Ha, Y. E. Goldman, P. R. Selvin: Myosin V walks hand-over-hand: single fluorophore imaging with 1.5-nm localization. *Science* 300, 2061-2065 (2003)
24. Walker M. L., S. A. Burgess, J. R. Sellers, F. Wang, J. A. Hammer, J. Trinick, P. J. Knight: Two-headed binding of a processive myosin to F-actin. *Nature* 405, 804-807 (2000)
25. Burgess S., M. Walker, F. Wang, J. R. Sellers, H. D. White, P. J. Knight, J. Trinick: The prepower stroke conformation of myosin V. *J Cell Biol* 159, 983-991 (2002)
26. Wang F., K. Thirumurugan, W. F. Stafford, J. A. Hammer, P. J. Knight, J. R. Sellers: Regulated conformation of Myosin V. *J Biol Chem* 279, 2333-2336 (2003)
27. Coureux P. D., A. L. Wells, J. Menetrey, C. M. Yengo, C. A. Morris, H. L. Sweeney, A. Houdusse: A structural state of the myosin V motor without bound nucleotide. *Nature* 425, 419-423 (2003)
28. Warshaw D. M., G. G. Kennedy, S. S. Work, E. B. Kremetsova, S. Beck, K. M. Trybus: Differential labeling of myosin V heads with quantum dots allows direct visualization of hand-over-hand processivity. *Biophys J* 88, L30-L32 (2005)
29. Sakamoto T., F. Wang, S. Schmitz, Y. Xu, Q. Xu, J. E. Molloy, C. Veigel, J. R. Sellers: Neck length and processivity of myosin V. *J Biol Chem* 278, 29201-29207 (2003)

## Five models for myosin V

30. Baker J. E., E. B. Krementsova, G. G. Kennedy, A. Armstrong, K. M. Trybus, D. M. Warshaw: Myosin V processivity: multiple kinetic pathways for head-to-head coordination. *Proc Natl Acad Sci USA* 101, 5542-5546 (2004)
31. Titus M. A.: Motor proteins: myosin V-the multi-purpose transport motor. *Curr Biol* 7, R301-R304 (1997)
32. Provance D. W., J. A. Mercer: Myosin-V: head to tail. *Cell Mol Life Sci* 56, 233-242 (1999)
33. Desnos C., S. Huet, F. Darchen: 'Should I stay or should I go?': myosin V function in organelle trafficking. *Biol Cell* 99, 411-423 (2007)
34. Trybus K. M.: Myosin V from head to tail. *Cell and Mol Life Sci* 65, 1378-1389 (2008)
35. Sellers J. R., L. S. Weisman: Myosin V. In: *Myosins: A Superfamily of Molecular Motors*, Ed: Coluccio L. M., *Proteins and Cell Regulation* 7, 289-323, Springer Netherlands (2008)
36. Taylor K. A.: Regulation and recycling of myosin V. *Curr Opin Cell Biol* 19, 67-74 (2007)
37. Sweeney H. L., A. Houdusse: The motor mechanism of myosin V: insights for muscle contraction. *Philos Trans R Soc Lond B Biol Sci* 359, 1829-1841 (2004)
38. Vale R. D.: Myosin V motor proteins: marching stepwise towards a mechanism. *J Cell Biol* 163, 445-450 (2003)
39. Sellers J. R., C. Veigel: Walking with myosin V. *Curr Opin Cell Biol* 18, 68-73 (2006)
40. Mehta A.: Myosin learns to walk. *J Cell Sci* 114, 1981-1998 (2001)
41. Tyska M. J., M. S. Mooseker: Myosin-V motility: these levers were made for walking. *Trends Cell Biol* 13, 447-451 (2003)
42. Olivares A. O., E. M. De La Cruz: Holding the reins on myosin V. *Proc Natl Acad Sci USA* 102, 13719-13720 (2005)
43. Schmitz S., J. Smith-Palmer, T. Sakamoto, J. R. Sellers, C. Veigel: Walking mechanism of the intracellular cargo transporter myosin V. *J Phys: Condensed Matter* 18, S1943-S1956 (2006)
44. Kolomeisky A. B., M. E. Fisher: A simple kinetic model describes the processivity of myosin-V. *Biophys J* 84, 1642-1650 (2003)
45. Vilfan A.: Elastic lever-arm model for myosin V. *Biophys J* 88, 3792-3805 (2005)
46. Lan G., S. X. Sun: Dynamics of myosin-V processivity. *Biophys J* 88, 999-1008 (2005)
47. Skau K. I., R. B. Hoyle, M. S. Turner: A kinetic model describing the processivity of myosin-V. *Biophys J* 91, 2475-2489 (2006)
48. Wu Y., Y. Q. Gao, M. Karplus: A kinetic model of coordinated myosin V. *Biochemistry* 46, 6318-6330 (2007)
49. Dunn A. R., J. A. Spudich: Dynamics of the unbound head during myosin V processive translocation. *Nat Struct Mol Biol* 14, 246-248 (2007)
50. Shiroguchi K., K. Kinoshita Jr: Myosin V walks by lever action and Brownian
51. Mehta A. D., R. S. Rock, M. Rief, J. A. Spudich, M. S. Mooseker, R. E. Cheney: Myosin-V is a processive actin-based motor. *Nature* 400, 590 (1999)
52. Cappello G., P. Pierobon, C. Symonds, L. Busoni, J. C. Gebhardt, M. Rief, J. Prost: Myosin V stepping mechanism. *Proc Natl Acad Sci USA* 104, 15328-15333 (2007)
53. Kolomeisky A. B., E. B. Stukalin, A. A. Popov: Understanding mechanochemical coupling in kinesins using first-passage-time processes. *Phys Rev E* 71, 031902 (2005)
54. Kad N. M., K. M. Trybus, D. M. Warshaw: Load and Pi control flux through the branched kinetic cycle of myosin V. *J Biol Chem* 284, 17477-17484
55. Hodges A. R., E. B. Krementsova, K. M. Trybus: Engineering the processive run length of Myosin V. *J Biol Chem* 282, 27192-27197 (2007)
56. Trybus K. M., E. Krementsova, Y. Freyzon: Kinetic characterization of a monomeric unconventional myosin V construct. *J Biol Chem* 274, 27448-27456 (1999)
57. Wang F., L. Chen, O. Arcucci, E. V. Harvey, B. Bowers, Y. Xu, J. A. Hammer, J. R. Sellers: Effect of ADP and ionic strength on the kinetic and motile properties of recombinant mouse myosin V. *J Biol Chem* 275, 4329-4335 (2000)
58. Forgacs E., S. Cartwright, M. Kovacs, T. Sakamoto, J. R. Sellers, J. E. Corrie, M. R. Webb, H. D. White: Kinetic mechanism of myosinV-S1 using a new fluorescent ATP analogue. *Biochemistry* 45, 13035-13045 (2006)
59. Rosenfeld S. S., H. L. Sweeney: A model of myosin V processivity. *J Biol Chem* 279, 40100-40111 (2004)
60. Yengo C. M., H. L. Sweeney: Functional role of loop 2 in myosin V. *Biochemistry* 43, 2605-2612 (2004)
61. Forgacs E., S. Cartwright, T. Sakamoto, J. R. Sellers, J. E. T. Corrie, M. R. Webb, H. D. White: Kinetics of ADP dissociation from the trail and lead heads of actomyosin V

## Five models for myosin V

following the power stroke. *J Biol Chem* 283, 766-773 (2008)

62. Purcell T. J., H. L. Sweeney, J. A. Spudich: A force-dependent state controls the coordination of processive myosin V. *Proc Natl Acad Sci USA* 102, 13873-13878 (2005)

63. Veigel C., S. Schmitz, F. Wang, J. R. Sellers: Load-dependent kinetics of myosin-V can explain its high processivity. *Nat Cell Biol* 7, 861-869 (2005)

64. Oguchi Y., S. V. Mikhailenko, T. Ohki, A. O. Olivares, E. M. De La Cruz, S. Ishiwata: Load-dependent ADP binding to myosins V and VI: Implications for subunit coordination and function. *Proc Natl Acad Sci USA* 105, 7714-7719 (2008)

65. Snyder G. E., T. Sakamoto, J. A. Hammer, J. R. Sellers, P. R. Selvin: Nanometer localization of single green fluorescent proteins: evidence that myosin V walks hand-over-hand via telemark configuration. *Biophys J* 87, 1776-1783 (2004)

66. Toprak E., J. Enderlein, S. Syed, S. A. McKinney, R. G. Petschek, T. Ha, Y. E. Goldman, P. R. Selvin: Defocused orientation and position imaging (DOPI) of myosin V. *Proc Natl Acad Sci USA* 103, 6495-6499 (2006)

67. Syed S., G. E. Snyder, C. Franzini-Armstrong, P. R. Selvin, Y. E. Goldman: Adaptability of myosin V studied by simultaneous detection of position and orientation. *EMBO J* 25, 1795-1803 (2006)

68. Schnitzer M. J., S. M. Block: Kinesin hydrolyses one ATP per 8-nm step. *Nature* 388, 386-390 (1997)

69. Fisher M. E., A. B. Kolomeisky: Simple mechanochemistry describes the dynamics of kinesin molecules. *Proc Natl Acad Sci USA* 98, 7748-7753 (2001)

70. Itoh H., A. Takahashi, K. Adachi, H. Noji, R. Yasuda, M. Yoshida, K. Kinosita: Mechanically driven ATP synthesis by F1-ATPase. *Nature* 427, 465-468 (2004)

71. Carter N. J., R. A. Cross: Mechanics of the kinesin step. *Nature* 435, 308-312 (2005)

72. Köhler J., G. Winkler, I. Schulte, T. Scholz, W. McKenna, B. Brenner, elasticity. *Proc Natl Acad Sci USA* 99, 3557-3562 (2002)

73. Ganoth A., E. Nachliel, R. Friedman, M. Gutman: Myosin V Movement: Lessons from Molecular Dynamics Studies of IQ Peptides in the Lever Arm. *Biochemistry* (2007)

74. Lan G., S. X. Sun: Flexible light-chain and helical structure of F-actin explain the movement and step size of myosin-VI. *Biophys J* 91, 4002-4013 (2006)

75. Kolomeisky A. B., M. E. Fisher: Molecular motors: a theorist's perspective. *Annu Rev Phys Chem* 58, 675-695 (2007)

76. Tsygankov D., M. E. Fisher: Kinetic models for mechanoenzymes: Structural aspects under large loads. *J Chem Phys* 128, 015102 (2008)

77. Huxley A. F.: Muscle structure and theories of contraction. *Prog Biophys Biophys Chem* 7, 255-318 (1957)

78. Hill T. L.: Theoretical formalism for the sliding filament model of contraction of striated muscle. Part I. *Prog Biophys Mol Biol* 28, 267-340 (1974)

79. Vilfan A., T. Duke: Instabilities in the transient response of muscle. *Biophys J* 85, 818-826 (2003)

80. Schwarzl S. M., J. C. Smith, S. Fischer: Insights into the chemomechanical coupling of the myosin motor from simulation of its ATP hydrolysis mechanism. *Biochemistry* 45, 5830-5847 (2006)

81. Koppole S., J. C. Smith, S. Fischer: Simulations of the myosin II motor reveal a nucleotide-state sensing element that controls the recovery stroke. *J Mol Biol* 361, 604-616 (2006)

82. Yu H., L. Ma, Y. Yang, Q. Cui: Mechanochemical coupling in the myosin motor domain. I. Insights from equilibrium active-site simulations. *PLoS Comput Biol* 3, e21 (2007)

83. Fischer S., B. Windshugel, D. Horak, K. C. Holmes, J. C. Smith: Structural mechanism of the recovery stroke in the myosin molecular motor. *Proc Natl Acad Sci USA* 102, 6873-6878 (2005)

84. Koppole S., J. C. Smith, S. Fischer: The structural coupling between ATPase activation and recovery stroke in the myosin II motor. *Structure* 15, 825-837 (2007)

85. Smith D. A.: How processive is the myosin-V motor? *J Muscle Res Cell Motil* 25, 215-217 (2004)

86. Schilstra M. J., S. R. Martin: An elastically tethered viscous load imposes a regular gait on the motion of myosin-V. Simulation of the effect of transient force relaxation on a stochastic process. *J R Soc Interface* 3, 153-165 (2006)

87. Vilfan A., E. Frey, F. Schwabl: Elastically coupled molecular motors. *Eur Phys J B* 3, 535-546 (1998)

88. Klumpp S., R. Lipowsky: Cooperative cargo transport by several molecular motors. *Proc Natl Acad Sci USA* 102, 17284-17289 (2005)

## Five models for myosin V

89. Svoboda K., P. P. Mitra, S. M. Block: Fluctuation analysis of motor protein movement and single enzyme kinetics. *Proc Natl Acad Sci USA* 91, 11782-11786 (1994)
90. Howard J., J. A. Spudich: Is the lever arm of myosin a molecular elastic element? *Proc Natl Acad Sci USA* 93, 4462-4464 (1996)
91. Vilfan A.: Influence of fluctuations in actin structure on myosin V step size. *J Chem Inf Model* 45, 1672-1675 (2005)
92. Vilfan A.: Myosin V passing over Arp2/3 junctions: branching ratio (2008)
93. Ali M. Y., E. B. Krementsova, G. G. Kennedy, R. Mahaffy, T. D. Pollard, K. M. Trybus, D. M. Warshaw: Myosin Va maneuvers through actin intersections and diffuses along microtubules. *Proc Natl Acad Sci USA* 104, 4332-4336 (2007)
94. Houdusse A., H. L. Sweeney: Myosin motors: missing structures and hidden springs. *Curr Opin Struct Biol* 11, 182-194 (2001)
95. Holmes K. C., I. Angert, F. J. Kull, W. Jahn, R. R. Schroder: Electron cryo-microscopy shows how strong binding of myosin to actin releases nucleotide. *Nature* 425, 423-427 (2003)
96. Conibear P. B., C. R. Bagshaw, P. G. Fajer, M. Kovacs, A. Malnasi-Csizmadia: Myosin cleft movement and its coupling to actomyosin dissociation. *Nat Struct Biol* 10, 831-835 (2003)
97. Reubold T. F., S. Eschenburg, A. Becker, F. J. Kull, D. J. Manstein: A structural model for actin-induced nucleotide release in myosin. *Nat Struct Biol* 10, 826-830 (2003)
98. Coureux P. D., H. L. Sweeney, A. Houdusse: Three myosin V structures delineate essential features of chemo-mechanical transduction. *EMBO J* 23, 4527-4537 (2004)

**Key Words:** Motor proteins, Motility, Myosin-V, Actin, Processivity, Mechano-chemical models, Discrete stochastic models, Chemical kinetics, Review

**Send correspondence to:** Andrej Vilfan, J. Stefan Institute, Jamova 39, 1000 Ljubljana, Slovenia, Tel: 386-1-477-3874, Fax: 386-1-4773-191, E-mail: [andrej.vilfan@ijs.si](mailto:andrej.vilfan@ijs.si)

<http://www.bioscience.org/current/vol14.htm>